

SMALL ANGLE X-RAY SCATTERING STUDIES OF REVERSE  
MICELLES IN SUPERCRITICAL FLUIDS

D. M. Pfund  
J. L. Fulton

October 1994

Presented at the  
Third International Symposium on Supercritical  
Fluids Conference  
October 17-19, 1994  
Strasbourg, France

Prepared for  
the U.S. Department of Energy  
under Contract DE-AC06-76RLO 1830

Pacific Northwest Laboratory  
Richland, Washington 99352

**MASTER**

## **DISCLAIMER**

This report was prepared as an account of work sponsored by an agency of the United States Government. Neither the United States Government nor any agency thereof, nor any of their employees, make any warranty, express or implied, or assumes any legal liability or responsibility for the accuracy, completeness, or usefulness of any information, apparatus, product, or process disclosed, or represents that its use would not infringe privately owned rights. Reference herein to any specific commercial product, process, or service by trade name, trademark, manufacturer, or otherwise does not necessarily constitute or imply its endorsement, recommendation, or favoring by the United States Government or any agency thereof. The views and opinions of authors expressed herein do not necessarily state or reflect those of the United States Government or any agency thereof.

## **DISCLAIMER**

**Portions of this document may be illegible in electronic image products. Images are produced from the best available original document.**

## **SUMMARY**

The nature of the aggregates formed in a supercritical fluid determines its solvent power and selectivity. Small angle x-ray scattering (SAXS) is a powerful tool for studying the properties of aggregates with sizes in the 10Å to 200Å range. It is also useful in studying those interparticle interactions which operate over a similar distance. We have used SAXS to examine the aggregates formed in pure fluids, in mixtures and in fluid/surfactant/water systems. The scattered intensity as a function of angle depends on the geometry, polydispersity, x-ray contrast, and interaction strength of the particles as well as on the phase behavior of the system. In this paper we present the results of modeling the x-ray scattering from AOT/water reverse micelles in supercritical propane and in propane/carbon dioxide mixtures. We examine the effect of dilution with CO<sub>2</sub> anti-solvent on the phase behavior of the system and on the strength of intermicellar attractions.

## **I. INTRODUCTION**

Reverse micelles and microemulsions are known to form in solvents that are above their critical points [1-3]. Although the properties of micelles formed in supercritical fluids have been studied by a number of different techniques, fundamental questions still remain about the thermodynamic and molecular parameters which govern the stability of the microemulsion and the structure of the micelles [4]. The interdroplet attractive force has been postulated as being due to short-ranged interactions between the tails of surfactant molecules and alternatively, as being due to long-ranged dispersion interactions between the micelle cores [5-7]. A better understanding of these systems must be obtained before the applications of supercritical reverse micelle systems to extractions, reactions, and enhanced oil recovery can be fully developed. Carbon dioxide is a desirable solvent for many supercritical fluid applications. However it is difficult to form reverse micelles in this fluid. In this work, we have estimated the size, polydispersity and the strength and range of intermicellar interactions in the AOT/water/supercritical propane system. In addition, we have examined the effect that small amounts of added carbon dioxide have on these properties.

## **II. EXPERIMENTAL**

The SAXS cell used in this work has been described previously [8]. The data were acquired on the Time-Resolved Diffraction Facility (station X12B) at the National Synchrotron Light Source (Brookhaven National Laboratory) in the manner also discussed previously. For these experiments, the incident wavelength was 1.38Å and the path length through the sample was 1.96 mm. The data from each experiment were scaled to a common incident beam intensity and to 100% transmission using the methods from the previous work [8]. Each scattering intensity curve  $I(q)$  (where  $q=(4\pi/\lambda) \sin(\theta/2)$  and  $\theta$  is the scattering angle) was on an arbitrary scale because both the incident photon flux and the x-ray contrast of the reverse micelles were unknown.

The surfactant AOT was obtained from Fluka (with purity >98%) and was further purified by the method of Kotlarchyk et al. [9]. The molar water-to-surfactant ratio (W) was 0.6 in the dried solid as determined by Karl Fischer titration. The propane and carbon dioxide were research grade from Scott and were used as received. The view cell solution was prepared by introducing the weighed solid AOT through a fitting in the cell. For these experiments the water-to-surfactant molar ratio was 12.0. Solvent was then added to increase the pressure to approximately 400 bar. A series of experiments was performed by venting fluid from the cell in stages to lower the pressure until the phase boundary was reached. For

the experiments which used the mixed propane/carbon dioxide solvent, low pressure carbon dioxide was introduced into the cell prior to increasing the pressure with pure propane. The carbon dioxide mole fraction in the solvent was approximately 0.05. All of the experiments described here were performed at a temperature of 110°C.

Each scattering curve consisted of a number of contributions including the scattering from AOT reverse micelles. The scattering from the empty cell was determined and subtracted, yielding the scattering from the sample itself. Scattering from solvent was measured at each temperature and pressure. Solvent scattering was then subtracted from each AOT/water/solvent scattering curve in proportion to the volume fraction of solvent in the mixture. Assuming that the solvent can be treated as a continuum, the resulting scattering curves contained contributions solely from the reverse micelles and their interactions. There remained a residual background scattering due to contributions from internal structures of molecular size within the micelles. This residual background for each experiment was estimated from a Porod plot of the data which was then subtracted to yield the final scattering curves for each experiment [8,10].

### III. MODEL

The final scattering intensity curves were described using a polydisperse model of interacting particles [11,12]:

$$I^{eu}(q) = \int_0^{\infty} f^2(q;D)\rho(D) dD + \iint_0^{\infty} f(q;D_1)f(q;D_2)\rho(D_1)\rho(D_2) i(q;D_1,D_2)dD_1dD_2 \quad (1)$$

The first integral, which gives the scattering in the absence of particle interactions, is taken over all possible particle diameters  $D$ . The second integral results from interparticle interference and is taken over all possible pairs of diameters  $D_1$  and  $D_2$ . In equation (1),  $I^{eu}$  is the intensity per unit volume in absolute electron units,  $\rho(D)$  is the particle size distribution function (normalized to the number density),  $f(q;D)$  is the scattering amplitude, and the structure factor  $i(q;D_1,D_2)$ , is a modified Fourier transform of the radial distribution function,

$$i(q;D_1,D_2) = \int_0^{\infty} [g(r;D_1,D_2) - 1] \frac{\sin(qr)}{qr} 4\pi r^2 dr \quad (2)$$

where the integral is over all possible center-to-center distances  $r$  between particles. The polydisperse formulation allows for modeling of the lack of pronounced minima in the scattering curves at larger angles. It also automatically accounts for the large and variable solubility of water in the supercritical solvent under the conditions being examined. The size distribution was assumed to be approximately Gaussian, with the tail at negative diameters being truncated (the exact nature of the function for small diameters is unimportant since such particles contribute little to the scattering curve). The integrations over particle diameter were carried out to a maximum of 3.5 standard deviations above the mean. The scattering amplitude was given by the Rayleigh expression for homogeneous spheres [10] where the spheres of various sizes were assumed to have equal x-ray contrast. The indicated particle diameters were approximately the overall diameters of the micelles because the electron density of the supercritical solvent was low. An analytical expression for  $i(q;D_1,D_2)$  was determined by

assuming a square well interaction potential and utilizing the fact that micelle concentrations were low, thereby allowing the radial distribution function to be replaced by the Boltzmann factor. The low concentration approximation was tested using Percus-Yevick theory and found to be acceptable. The diameter of the repulsive core was assumed to be equal the same diameter of the micelle which appears in the scattering amplitude. The well width and well depth were assumed to be approximately independent of particle diameter. The resulting square well potential is an approximation of the potential of mean force between micelles in the McMillan-Meyer description of the solvent. A conversion factor was used (its determination is discussed below) to convert the calculated intensities in electron units to intensities in (arbitrary) experimental units.

**Figure 1.** Contribution of intermicellar structure factors to the total intensity in propane.

The structure factors were non-zero only for  $q$ -values less than about  $0.125 \text{ \AA}^{-1}$ . Figure 1 illustrates the contribution of the structure factors to the intensity as a function of  $q$ . Thus, the determination of model parameters by non-linear regression was a two step process. The mean size, standard deviation and the product of the number density and an intensity conversion factor were determined from data at  $q$  greater than  $0.125 \text{ \AA}^{-1}$ . Over this high  $q$ -range the intensities were given solely by the first integral in equation (1). The intensity conversion factor could only be determined independently from the number density when interparticle interference (given by the second integral) was large. The well width and depth, and the intensity conversion factor were determined from data at  $q$  less than  $0.175 \text{ \AA}^{-1}$ . The size distribution parameters were also recalculated as the square well parameters were optimized, but in practice the former did not change significantly. The well-depth and intensity conversion factor were partially coupled parameters, but this coupling was weak when the well depth was shallow (as was found to be true in this work).

#### IV. RESULTS AND DISCUSSION

Plotted in Figure 2 are scattering intensities as a function of  $q$  in the propane solvent at pressures of 400 bar and 250 bar. The phase boundary was at a pressure of about 220 bar. There was little change in the particle size distribution as the pressure was reduced. The mean particle diameter ( $32 \text{ \AA}$ ), standard deviation ( $15.5 \text{ \AA}$ ) and number density ( $3.0 \times 10^{-6} / \text{ \AA}^3$ ) all remained constant. The increases in scattering at small  $q$ -values were caused by changes in the structure factor with decreasing pressure. The change in x-ray contrast (as measure by changes in the intensity conversion factor) was small. The micelle-micelle interactions were long-ranged. As pressure was varied the range of the effective pair potential, as measured by the well width, was approximately constant at  $52\text{-}53 \text{ \AA}$  away from the surface of the core. The well depth increased as pressure was reduced from  $0.084 \text{ kT}$  at 400 bar to  $0.163 \text{ kT}$  at 250 bar.

**Figure 2.** The change in the scattering intensity function as pressure is reduced. The solvent is propane.

The results obtained using the mixed propane/carbon dioxide solvent were quite different. Plotted in Figure 3 are scattering intensities as a function of  $q$  in the mixed solvent at pressures of 400 bar, 300 bar and 225 bar. The phase boundary was again at a pressure of about 220 bar. Scattering at all angles was changed as pressure was reduced. Scattering at

small angles increased as pressure was reduced between 400 bar and 300 bar, as in the propane system. Further reductions in pressure caused a loss in intensity at small angles. This loss of intensity was not caused by changes in the intermicellar interactions. Plotted in Figure 4 are the particle contributions to the scattering (the first integral in equation 1) at 300 bar and 225 bar in the mixed solvent system. Further analysis will determine whether this change was caused by changes in the particle size distribution or by reduction in the x-ray contrast. Truth of the first hypothesis would suggest that carbon dioxide interferes with micellar formation.

**Figure 3.** The change in the scattering intensity function as pressure is reduced. The solvent is mixed propane/carbon dioxide.

## V. CONCLUSIONS

Micelle-micelle interactions were weak and long-ranged in the AOT/water/supercritical propane system at 110°C. The strength of intermicellar attraction increased at lower pressure. The particle size distribution in this system was independent of pressure. Introducing carbon dioxide into the solvent produced changes in the pressure dependence of the particle scattering. These changes suggest either that there was a loss of x-ray contrast near the phase boundary or that carbon dioxide interferes with micelle formation equilibrium. Work is in progress that will provide more detailed information about the pressure dependence of the size distribution and about the micellar interactions in this mixed solvent system.

**Figure 4.** Particle scattering intensity in the mixed solvent system.

## VI. ACKNOWLEDGMENT

This research was supported by the Director, Office of Energy Research, Office of Basic Energy Sciences, Chemical Sciences Division of the U.S. Department of Energy, under contract DE-AC06-76RLO 1830.

## VII. REFERENCES

- [1] Fulton, J.L.; Smith, R.D. *J. Phys. Chem.* **1988**, *92*, 2903-2907.
- [2] Smith, R.D.; Fulton, J.L.; Blitz, J.P.; Tingey, J.M. *J. Phys. Chem.* **1990**, *94*, 781-787.
- [3] Johnston, K.P.; McFann, G.J.; Lemert, R.M. In *Supercritical Fluid Science and Technology*; Johnston, K.P., Penninger, J.L.M., Eds.; ACS Symposium Series No. 406: Washington, 1989, p. 140.
- [4] Chen, S.H.; *Ann. Rev. Phys. Chem.* **1986**, *37*, 351-399.
- [5] Huang, J.S.; *J. Chem. Phys.* **1985**, *82*, 480-484.
- [6] Kaler, E.W.; Billman, J.F.; Fulton, J.L.; Smith, R.D. *J. Phys. Chem.* **1991**, *95*, 458-462.
- [7] Lemaire, B.; Bothoral, P.; Roux, D. *J. Phys. Chem.* **1983**, *87*, 1023.
- [8] Carnahan, N.F.; Quintero, L.; Pfund, D.M.; Fulton, J.L.; Smith, R.D.; Capel, M.; Leontaritis, K. *Langmuir* **1993**, *9*, 2035-2044.
- [9] Kotlarchyk, M.; Chen, S.H.; Huang, J.S.; Kim, M.W. *Phys. Rev. A* **1984**, *29*, 2054.
- [10] Glatter, O.; Kratky, O.; Eds. *Small Angle X-Ray Scattering*; Academic Press: New York, 1982.
- [11] van Beurten, P.; Vrij, A. *J. Chem. Phys.* **1981**, *74*, 2744-2748.
- [12] Pitre, F.; Regnaut, C.; Pileni, M.P. *Langmuir* **1993**, *9*, 2855-2860.

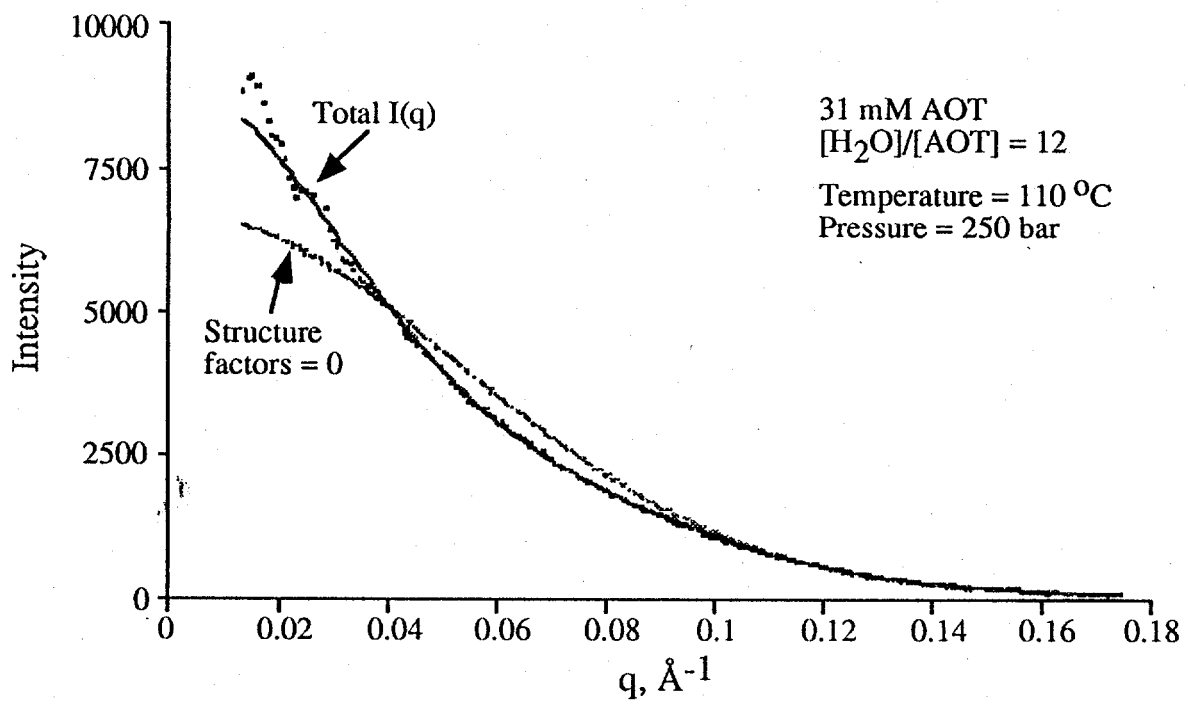


figure 1

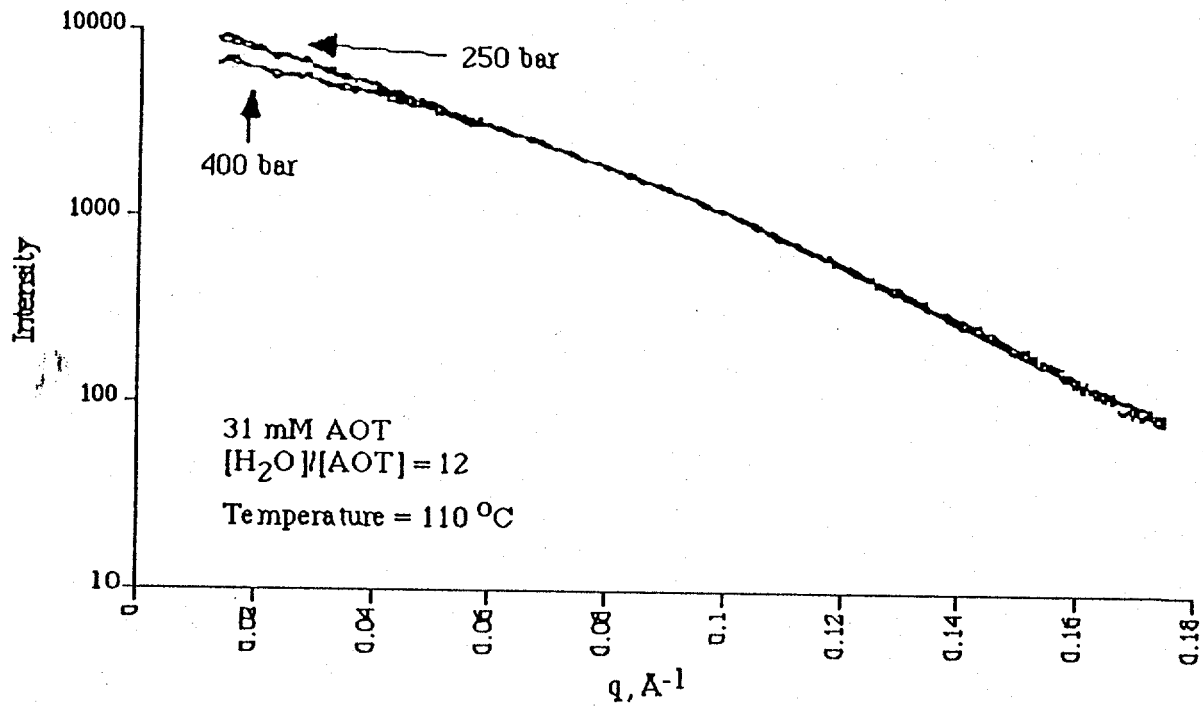


Figure 2

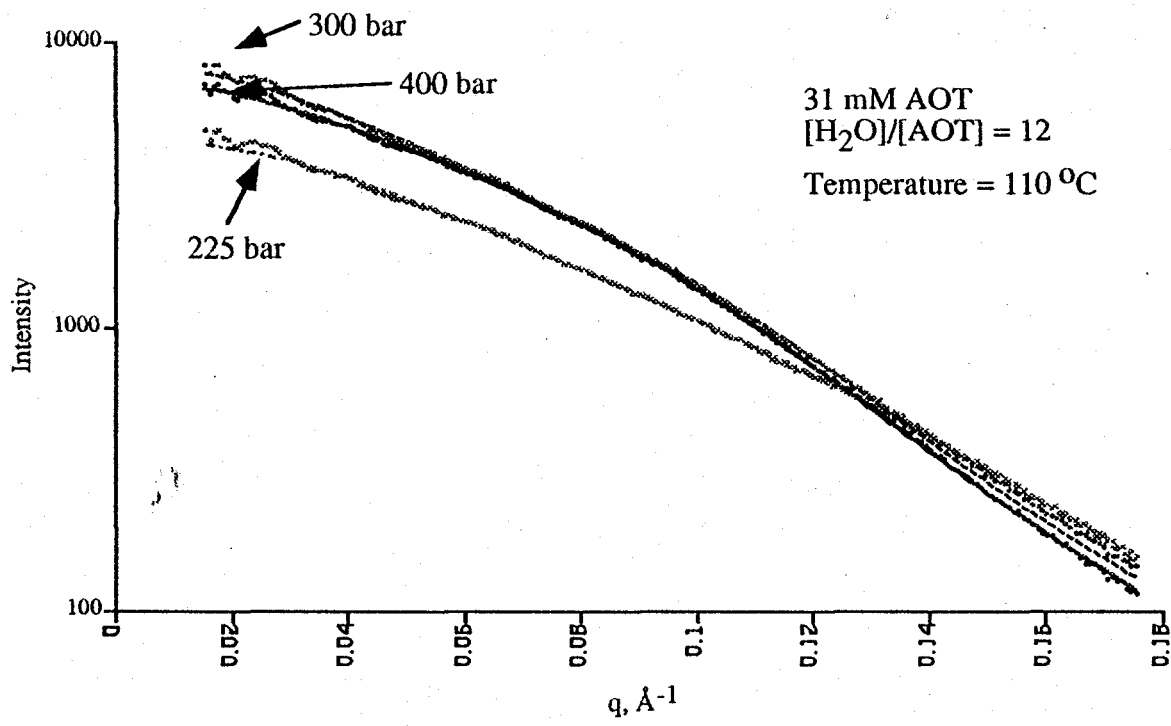


figure 3

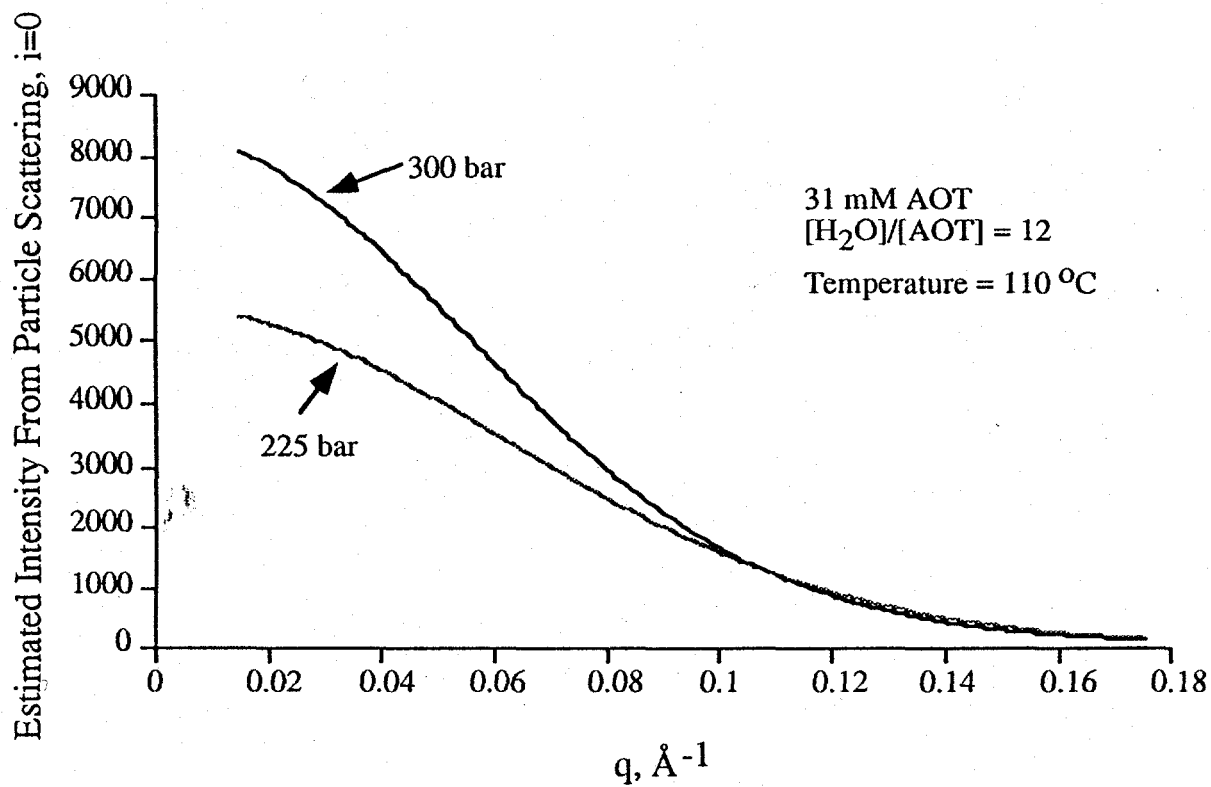


Figure 4